0273-2289/03/104/0081/$20.00

Effect of Mn^{2+}, Co^{2+}, Ni^{2+}, and Cu^{2+} on Horseradish Peroxidase

Activation, Inhibition, and Denaturation Studies

A. Mahmoudi,[1,2] K. Nazari,[3] N. Mohammadian,[2] and A. A. Moosavi-Movahedi*,[1]

[1]Institute of Biochemistry and Biophysics, University of Tehran, Tehran, Iran, E-mail: moosavi@ibb.ut.ac.ir; [2]Chemistry Department, Tehran Northern Branch, Islamic Azad University, Tehran, Iran; and [3]Inhibitors Department, Research Institute of Petroleum Industry, N.I.O.C., Tehran, Iran

Received August 1, 2001; Revised May 1, 2002; Accepted May 1, 2002

Abstract

The effects of transition metal ions (M^{2+}) such as Mn^{2+}, Co^{2+}, Ni^{2+}, and Cu^{2+} on the functional and structural stabilities of horseradish peroxidase (HRP) were investigated with respect to reversible chemical denaturation, Michaelis–Menten kinetics, chemical modification and time-dependent catalytic activity. Conformational Gibbs free energy ($\Delta G^{\circ}_{(H_2O)}$) as a structural stability criterion and transition concentrations of metal ions ($[M^{2+}]_{1/2}$) were estimated using a two-state chemical denaturation model. Activation and inhibitory concentration ranges for each metal ion were specified by the steady-state enzyme kinetics. Results of a pH-profile method confirmed by chemical modification indicate that a histidine residue interacts in the activation concentration range, whereas carboxylic residues (Asp and Glu) contribute to interaction in the inhibitory concentration range. Incubation of the enzyme with the metal ion at activation concentration leads to long-term functional stability of peroxidase. Thus, such metal ions as potent effectors induced the enhancement of conformational and functional stabilities of horseradish peroxidase.

Index Entries: Horseradish peroxidase; transition metal ions; activation; inhibition; denaturation; functional stability.

*Author to whom all correspondence and reprint requests should be addressed.

Introduction

Peroxidases are enzymes that catalyze oxidative reactions by decomposing hydrogen peroxide at the expense of various substrates, such as phenols and amides.

They have been isolated and purified from some organisms, including bacteria, fungi, and higher plants. There is great interest in horseradish peroxidase (HRP) for analytical, synthesis, and biotechnological purposes *(1)*.

The stability of a protein during isolation and purification processes and in operational conditions is of vital importance in biotechnology. Several strategies are at hand to increase operational stability of a protein: the use of stabilizing additives, immobilization, crystallization, and medium engineering. Earlier studies have also reported the stabilizing behavior of osmolytes on the structure and function of different enzymes and proteins *(2–11)*, which indicates the importance of such studies.

The stability of HRP has been studied from various points of views. These include long-term functional stability of HRP as a result of metal incubation *(12)* and works that are focused on the structural stability of HRP *(13–16)*. It has been reported that HRP contains two bound Ca^{2+}, which are important for both the activity and thermal stability of the protein, and the role of disulfide bonds and N-glycosylation sites in the structural stability of HRP has been investigated *(14,17–24)*. Parameters of structural stability for guanidine hydrochloride (Gdn–HCl) and urea *(14,25)* and surfactant-induced unfolding of HRP *(15)* and apo-HRP *(26)* have been obtained and compared with that of its similar homolog, cytochrome-*c* peroxidase *(14)*. Some reports have been published regarding the crystal structure of HRP *(23)* and its complexes with substrates *(27,28)*. The crystal structure of HRP and the horseradish peroxidase–benzhydroxamic acid (HRP-BHA) complex have been determined at 2.15 Å and 2.0 Å resolution, respectively *(23,28)*, in which benzhydroxamic acid (BHA) has been used as a probe for the aromatic donor-binding site *(27)*. They showed that BHA is located in the distal heme pocket, nearly parallel to the heme, but too far away to directly interact with the iron atom. The functional groups of BHA are held by hydrogen bonds to the N^{ε} of the distal His, the N^{ε} of the distal Arg, and the oxygen atom of a Pro residue (Pro139), and only H_2O molecule present in the cavity is located at 2.6–2.7 Å from the iron atom *(27)*.

There are some reports on the inhibitory behavior of transition metals on peroxidases that have been published previously *(29–32)*, and, recently, the effects of some metals on functional stability of peroxidase have been reported *(17)*. Here, we attempt to investigate the effect of Mn^{2+}, Co^{2+}, Ni^{2+}, and Cu^{2+} on the interaction with HRP in the presence of guaiacol as an aromatic donor on activation, inhibition, and denaturation.

Materials and Methods

Peroxidase from horseradish type II with a purity index of ($Abs_{403/275}$ = RZ) RZ ≈2.5 was provided by Merck. Hydrogen peroxide, guaiacol, chloride

salts of transition metals, and sodium phosphates ($NaH_2PO_4 \cdot H_2O$; $NaHPO_4 \cdot 2H_2O$) were also purchased from Merck. Woodward's reagent K (2-ethyl-5-phenyl isoxazolium-3-sulfonate, WRK) and diethylpyrocarbonate (DEPC) were obtained from Sigma. All solutions were prepared using deionized water (Barnstead NanoPure D4742; E.C. = 5.5×10^{-2} μs).

Spectrophotometric Titration of HRP Solution with Metal Ions

Chemical denaturation profiles were obtained using a Shimadzu 2101 spectrophotometer. Such titrations were carried out at 275 nm as a probe of conformational change of enzyme, known amounts of metal ion solution were added to the protein solution, and subsequent data were processed to evaluate stability parameters. An extinction coefficient of $1.02 \times 10^5 cm^{-1} M^{-1}$ at 403 nm *(33)* was used to calculate the concentration of protein. Details of experimental conditions are shown in the legends of the figures.

Kinetic Analysis

Steady-state kinetics of guaiacol oxidation by hydrogen peroxide catalyzed by HRP were obtained at 470 nm (color product of reaction) *(33)* in the presence and absence of various amounts of metals ions in 2.5 m*M* phosphate buffer, pH = 7.0.

Michaelis–Menten curves were obtained by using different concentrations of guaiacol at various concentrations of metal ions. The concentration of H_2O_2 was kept high and constant with respect to the hydrogen donor (AH) during the course of reaction to ensure pseudo-first-order condition. In a period of 30 s for recording the progress curves [HRP] = 4.6×10^{-8} *M*, [AH] = 0.2–8 m*M*, and [H_2O_2] = 0.25 m*M* were added, respectively, to a 1.5-mL cuvet and the initial rate of reaction (V_0) was calculated from the time domain of 15 s at the linear portion of curve. In order to reach the steady-state condition, a time delay of 7 s was used. H_2O_2 stock solutions were prepared by appropriate dilutions of 30% (v/v) H_2O_2 in deionized water. The concentrations of hydrogen peroxide were determined by absorbance measurements at 240 nm, using a ε_{240} of 43.6 $cm^{-1} M^{-1}$ *(34)*. The dilute solutions were prepared daily.

Modification of Histidine and Carboxylic Residues

Chemical modification of His and Asp/Glu residues were performed with DEPC and WRK reagents, respectively. Details of experimental procedures were similar to the works of Chauthaiwale and Rao *(35)* and Miles *(36)*.

Results and Discussion

In order to evaluate parameters of structural stability, the denaturation profiles of HRP by M^{2+} were monitored at 275 nm. The analysis was based on the two-state model by Pace and co-workers to determine the

Table 1
Parameters for Two-State Denaturation of HRP by Various Denaturants

Denaturant	$[D]_{1/2}$ (m*M*)	$\Delta G^\circ_{(H_2O)}$ (kJ/mol)	Molar percent of denaturation	$k_{int.}$ (M^{-1})	Δn (mmol)
Gdn-HCl[a]	1.9×10^3	26.02	100	0.6	97.8×10^3
Urea[a]	2.8×10^3	24.57	94.41	0.1	51.33×10^3
DTAB[b]	1.35	23.64	90.84	50	569
SDS[b]	1.15	23.66	90.91	50	360
Mn^{2+}	16.4	10.53	40.46	24.2	14.3
Co^{2+}	3.39	18.53	71.2	46.5	50.7
Ni^{2+}	28	9.45	36.31	6.36	24.3
Cu^{2+}	0.37	14	53.8	674.8	26.0

Note: $[D]_{1/2}$ is the transition concentration for 50% denaturation of molecular population of enzyme in the presence of denaturant.
[a]Data from ref. *20*.
[b]Data from ref. *10*.

transition concentration $[M^{2+}]_{1/2}$ and conformational stability ($\Delta G^\circ_{(H_2O)}$) *(15,25,37–39)*. Results obtained for Ni^{2+}/HRP are presented in detail. Similar results for the other metal ions are recorded in Tables 1 and 2.

At low concentrations of M^{2+} (e.g., ≤ 5 m*M* for Ni^{2+}) no considerable conformational change was detected (pretransition region), whereas at higher concentrations (> 5 m*M* for Ni^{2+}), gradual change of structure began. Denaturation was complete at about 50 m*M* of Ni^{2+}. Figure 1 shows a typical spectrophotometric titration of HRP with Ni^{2+} solution. The figure indicates the considerable interaction between HRP and a metal ion over a range of 0–50 m*M* of Ni^{2+}. This interaction, based on two-state reversible denaturation *(37)*, caused the conformational change of HRP structure that was measured by difference spectrophotometry at 275 nm (aromatic side chains). Electrostatic binding of metal ions to negative binding sites change the net charge of the surface of the protein to the positive state, and repulsion between these positive charges can lead to denaturation of the protein structure. This process becomes especially important at concentrations over $[D]_{1/2}$, although the extent of such denaturation is comparably mild when compared to Gdn–HCl denaturation. Thus, metal ions at high concentrations can convert the native enzyme structure to a partially denatured state (*see* Table 1).

By analyzing the sigmoidal curve, we can obtain stability parameters of interaction such as transition concentration $[M^{2+}]_{1/2}$ and Gibbs free energy of stability ($\Delta G^\circ_{(H_2O)}$). Monitoring the transition by means of a physical parameter like absorbency, we have the following:

$$\text{Native HRP (N)} \rightleftharpoons \text{Denatured HRP (D)} \qquad \text{(I)}$$

$$(\Delta G^\circ_D) = -RT \ln K_D = -\text{RT} \ln[(A_N - A_{obs})/(A_{bos} - A_D)] \qquad (1)$$

Table 2
Parameters for Activation and Competitive Inhibition of HRP by Metal Ions at 27°C and pH = 7.0 of 2.5 m*M* Phosphate Buffer

Metal ion		$[M^{2+}]$ (m*M*)	K'_m (m*M*)	K_I (m*M*)
Mn^{2+}*	*b*	0	2.178	
		0.2	4.03	
		0.4	5.42	0.318
		0.6	7.20	
Co^{2+}	*a*	0.0083	1.835	
		0.0124	1.810	
		0.0210	1.73	
	b	0.207	3.12	
		0.413	3.32	2.93
		0.620	3.36	
Ni^{2+}	*a*	1	1.856	
		2	1.891	
		3	1.958	
	b	5	2.26	
		6	2.34	23.25
		8	2.50	
Cu^{2+}	*a*	0.12	1.898	
		0.21	1.473	
		0.30	1.210	
	b	0.645	4.217	
		0.750	4.234	26.28
		0.800	4.257	

*For Mn^{2+}, activatory behavior was not detected.
[a]Activation. [b]Inhibition.

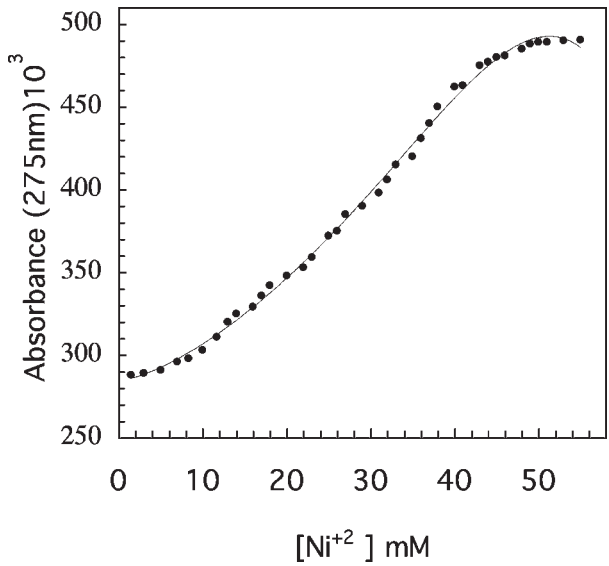

Fig. 1. Spectrophotometric titration of HRP solution by Ni^{2+} at 275 nm. Experimental conditions: 27°C, 2.5 m*M* phosphate buffer, pH = 7.0, [HRP] = 1×10^{-5} *M*.

where ΔG°_D is the standard free energy due to the denaturation process (reaction I) and K_D is the apparent equilibrium constant of the transition process [Eq. (1)], which depends on the concentration of metal ion. A_{obs}, A_N, and A_D are the observed absorbance, the absorbance of the native conformation, and absorbance of the denatured form, respectively. Plotting the ΔG°_D as a function of metal ion concentration according to the linear relation *(25)*

$$\Delta G^\circ_D = \Delta G^\circ_{(H_2O)} - m[M^{2+}] \quad (2)$$

provides a way for estimation of $\Delta G^\circ_{(H_2O)}$ as the *Y*-intercept and $[M^{2+}]_{1/2}$ as the – intercept/slope = $-m$ of the graph. On the basis of the denaturant binding model (DBM), which gives satisfactory results for binding of denaturants to proteins, the linear relation can also be written as follows *(38,39)*:

$$\Delta G^\circ_D = \Delta G^\circ_{(H_2O)} - \Delta nRT \ln(1 + k_{int}[M^{2+}]) \quad (3)$$

where Δn is the difference between the number of moles of denaturant bound to denatured and native conformations, R is the universal gas constant, and k_{int} is the intrinsic binding constant for binding of the denaturant to the respected sites on the protein molecule *(38)*. Using a common fitting software such as EUREKA, the experimental data (ΔG°_D and $[M^{2+}]$) are fitted to Eq. (3) and parameters $\Delta G^\circ_{(H_2O)}$, Δn, and k_{int} are obtained and recorded in Table 1.

Previous studies show that the native HRP conformation converts to a maximally denatured state when strong denaturants are used, such as urea, Gdn–HCl, or ionic surfactants *(14,15,25)*.

The native conformation of HRP has a conformational stability $\Delta G^\circ_{(H_2O)}$ of about 26 kJ/mol (free energy in the absence of denaturants) at 25°C and pH = 6.4 *(15,25)*. Comparing the $\Delta G^\circ_{(H_2O)}$ values of the enzyme structure results to the fact that metal ions convert the native form to the partially denatured conformation (*see* Table 1). Table 1 shows the extent of the denaturation process induced by metal ions; Gdn–HCl denaturation is selected as the reference point. Scheme I shows that the maximum structural unfolding occurs as a result of the effect of Gdn–HCl on the enzyme and other denaturants compared to Gdn–HCl and induces less unfolding in HRP conformation. From a thermodynamic point of view, Gdn–HCl as a potent denaturant is able to bring the protein conformation to a near fully unfolded state. Therefore, by selecting the $\Delta G^\circ_{(H_2O)}$ of Gdn–HCl as the reference point and assigning a value of 100 to it, the extent of denaturation is calculated as the percentage of denaturation for the other denaturants (e.g., metal ions), as shown in Table 1.

Co^{2+} and Cu^{2+} have high potential for binding to HRP, leading to a conformational change. Low transition concentrations ($[M^{2+}]_{1/2}$) corresponded to a greater Δn (extent of binding), causing partial denaturation of HRP to an extent of 71% and 54% for Co^{2+} and Cu^{2+}, respectively. (*See* Table 1 and Scheme I.)

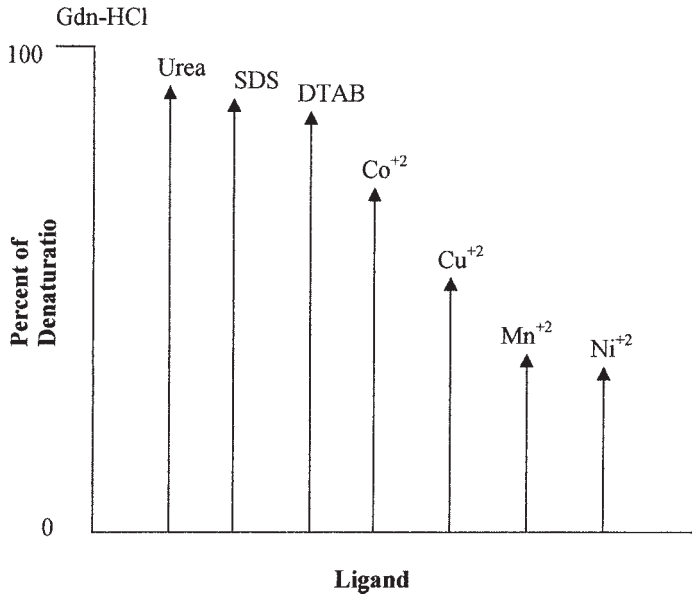

Scheme I. Maximum percentage of denaturation caused by different additives.

Similar effects for Ni^{2+} could be observed only at a high transition concentration of about 27 m*M*. From an industrial point of view, it means that the contamination of HRP solutions by small amounts of Co^{2+} and Cu^{2+} (in the range of transition concentration) leads to conformational change (partial denaturation) and inhibitory effects in the enzyme. Comparing k_{int} values (intrinsic binding constants for binding of metal ions on binding sites of protein) shows that Cu^{2+}, due to its high ionic potential *(28)*, has a quite different binding affinity with respect to the other metal ions. This is highlighted by the lower transition concentration ($[M^{2+}]_{1/2}$) for Cu^{2+} (0.37 m*M*).

Effects of M^{2+} on Steady-State Kinetics of HRP

In order to evaluate the effects of metal ions on the functional stability of the enzyme, the kinetics of enzyme catalysis was investigated in the presence of various concentrations of metal ions. Results show that metal ions at low concentrations have activatory behaviors, and at higher concentrations, they have inhibitory behaviors.

Using steady-state Michaelis–Menten kinetics, K_m and V_{max} values were estimated from the hyperbolic curves of the catalytic reaction cycle. Accurate determination of K_m (from the *X*-intercept) and V_{max} (from the *Y*-intercept) values were performed using linear Lineweaver–Burk plots *(40)*:

$$1/V = 1/V_{max} + (K_m/V_{max}) \times 1/[S] \quad (4)$$

In the presence of a reversible competitive inhibitor, the inhibitory constant (K_I) of the metal ion could be determined from the variation of

apparent K_m value (K'_m), with concentration of the inhibitor referred to as the "secondary plot" according to Eq. (6):

$$1/V = 1/V_{max} + (K'_m/V_{max}) \times 1/[S] \quad (5)$$

$$K'_m = K_m + (K_m/K_I)\,[\text{Inhibitor}] \quad (6)$$

By obtaining initial rates, followed by sketching appropriate Michaelis–Menten curves, and, finally, plotting double-reciprocal graphs (Lineweaver–Burk plots), K_m, V_{max}, and K'_m were obtained. Figure 2 shows typical Lineweaver–Burk plots for various concentrations of Ni^{2+} as described in the Materials and Methods section. Over a concentration range of 0–4 m*M*, an increasing Ni^{2+} concentration led to increased catalytic activity of HRP (corresponding to decreases in the values of K'_m). This concentration range (for each metal ion) was defined as the "activation concentration range." Over the concentration range of 5–8 m*M* of Ni^{2+}, at increasing metal ion concentration, K'_m values increased and this concentration range was defined as "the inhibitory concentration range." Activation and inhibitory concentration ranges of metal ions, along with their respected K_m values, are recorded in Table 2.

After finding the inhibitory concentrations for each metal, secondary plots for estimating K_I have been sketched for each metal ion (*see* Table 2). The inset in Fig. 2 shows a typical secondary plot for the inhibitory effect of Ni^{2+}.

Estimation of pK_a Values for Ni^{2+} Binding Sites

It was found that metal ions, at low concentrations, activate the enzyme (*see* Fig. 2). In order to specify which residues at the active site interact with Ni^{2+}, pH-profile and chemical modification experiments have been conducted.

Using the pH-profile technique, as a difference spectrophotometric method, the pK_a values of functional groups in the active site of HRP could be determined. In this method, changes in absorption when a ligand, such as a metal ion, is specifically bound to a binding site are sketched against pH. The peaks are produced corresponding to pK_a values of groups that interacted with the specific ligand. Further characterization of the interacting groups could be carried out using chemical modification of probable interacting residues. In order to evaluate such binding effects in the heme environment, the soret band absorption (λ_{max} = 403 nm) was selected for monitoring the interaction. Details of the technique are described and discussed in the literature *(41–43)*.

Interaction of M^{2+} with peroxidase is associated with perturbation of the heme soret absorption, which suggests that binding of M^{2+} takes place at the site close enough to the heme periphery to affect the electronic absorption spectrum of the heme group. Because activatory effects of metal ions relate to binding of the ion to residues in the active site, the pH-profile technique was used to identify the residues interacting with the metal ions

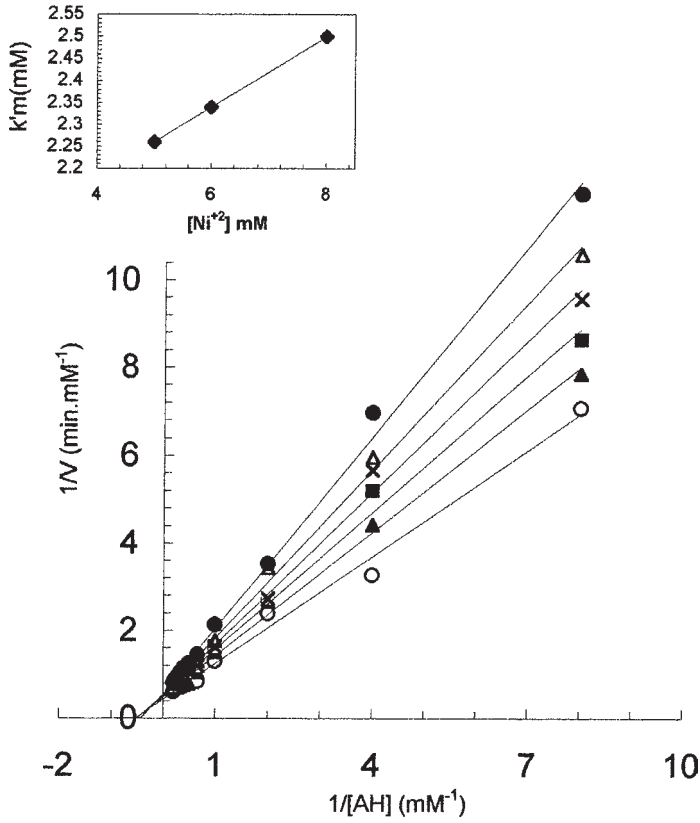

Fig. 2. Double-reciprocal plot of $1/V_0$ versus 1/[AH]. Before each experiment, a [HRP] = 3×10^{-7} *M* solution was incubated with various concentrations of Ni^{2+}. Five microliters of such solution was injected into the cell. The concentrations of HRP and H_2O_2 in the resulting reaction mixture are 1×10^{-9} *M* and 1×10^{-4} *M*, respectively, in 2.5 m*M* phosphate buffer at pH = 7.0 and 27°C; (○) with 1 m*M* Ni^{2+}, (▲) with 3 m*M* Ni^{2+}, (■) native HRP, (×) with 5 m*M* Ni^{2+}, (Δ) with 6 m*M* Ni^{2+}, (●) with 8 m*M* Ni^{2+}. The inset shows the plot for competitive inhibition of HRP by Ni^{2+}. Data according to Eq. (6) were used for the evaluation of K_I from the intercept of the graph.

(41). In accordance with this model, it is assumed that if an ionizing species in a protein molecule binds to a ligand such as a metal ion, substrate, or a coenzyme in a specific manner, the extent of charge on the interacting molecule will be changed as a function of ionization of the group under study. This effect could be transmitted to the adjacent absorbing chromophore (heme chromophore) that may be present in the molecule, in a position where it could be affected by it. This effect is, in fact, similar to the direct titration of the group and could be followed as a function of changing pH *(42,43)*. The plot of the difference in absorption on the specific binding of M^{2+} to a binding site versus the pH produces a peak corresponding to the pK_a value of the group that interacts with that specific ligand. Figure 3 shows pH profiles for activation (2 m*M*) and inhibitory (8 m*M*) concentrations of Ni^{2+}.

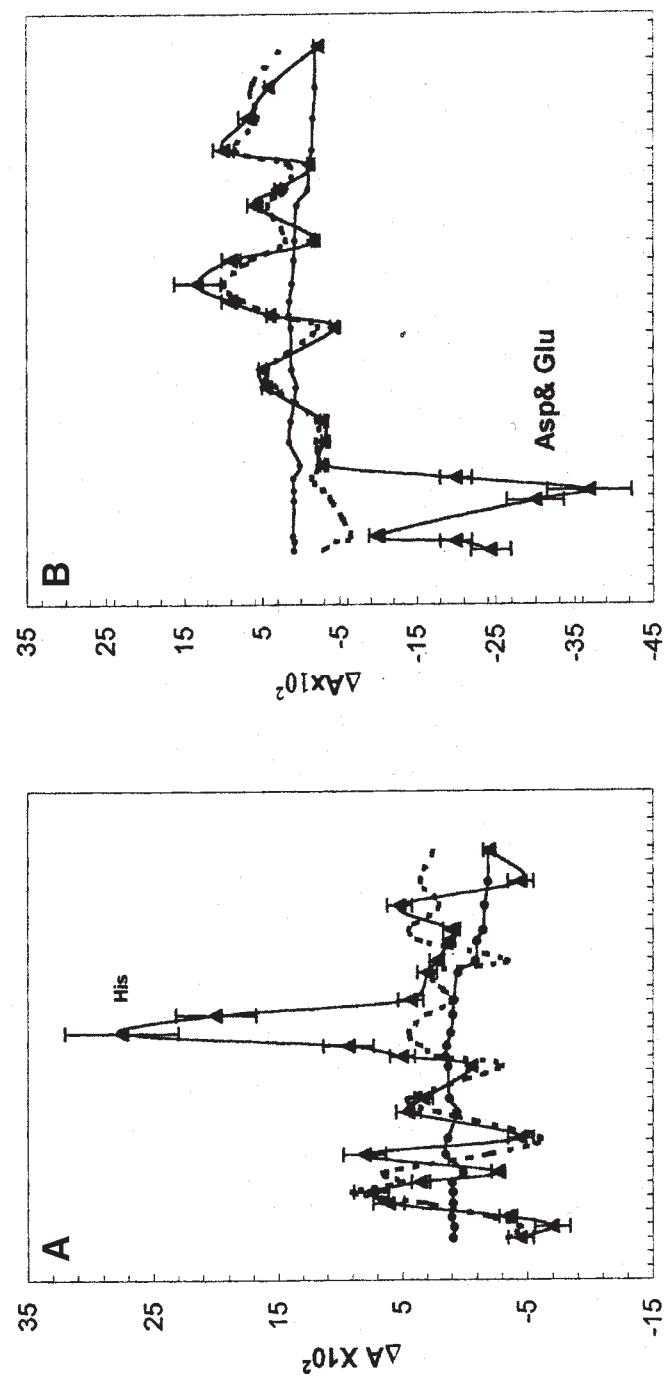

Fig. 3. pH profile for estimation of pK_a values of the interacting functional groups of HRP with Ni^{2+}. (●) Native HRP baseline (difference absorbance against phosphate buffer as the blank); (– – –) in the presence of specific modifiers (DEPC for His and WRK for carboxylic residues); (▲) in the presence of Ni^{2+}. For pH = 3–5, Tris-HCl, was used as the buffer for pH = 5.5–8, a phosphate buffer was used, and for pH > 8, basic Tris was used as the buffer; all in constant ionic strength of $I = 6.9 \times 10^{-3}$ *M*. **(A)** Activatory concentration of Ni^{2+} (4 m*M*); **(B)** inhibitory concentration of Ni^{2+} (8 m*M*).

The curve corresponding to the activation concentration shows two peaks over the pH range of 4–5, which may attributed to carboxylic residues. The sharp peak at pH = 6.5 likely corresponds to a histidine residue (imidazole side chain). In order to ensure this assignment, chemical modification of the imidazole group of histidine residues of HRP has been performed using the specific histidine modifier, diethylpyrocarbonate (DEPC) *(44,45)*. For the modified protein, the peak at pH = 6.5 was not evident, satisfying the idea that the interacting group with a pK_a = 6.5 is indeed a histidine residue. As shown in the literature, the interaction of transition metal ions with O-donor groups are much weaker than with N donors *(46)*. HRP has about 27 carboxylic residues; their overall weak interaction with Ni^{2+} were observed at the above-mentioned pH range. In Fig. 3, the curve corresponding to inhibitory concentration shows that in addition to histidine, acidic residues were also affected considerably. Modification of such carboxyl residues (Asp and Glu) with Woodward's reagent K *(35)* removed these sharp peaks. A similar observation was made for modified HRP upon interaction with a competitive inhibitor, benzhydroxamic acid *(45)*.

According to a previous report, HRP has only three His residues in its primary structure *(22)*. His170 occupies the fifth coordination position on the heme iron (proximal histidine) *(47,48)* and is not titratable. The distal histidine (His42) that is located at the distal side and close to the heme group has been known as a catalytic residue in the catalytic action of HRP *(45,48,49)*. This is why His42 is the interacting group with Ni^{2+}. Because the p*Ka* values were ascribed to protonation of distal His, the decrease of the p*Ka* value corresponds to less basicity of the His in the Ni^{2+}-incubated HRP. Thus, we propose that the distal His be required to be located at the optimal position for the essential hydrogen-bond network by the hydrogen bond to Asn70 for effective peroxidase catalysis.

On the other hand, the hydrogen bonds in the heme distal cavity improves the function of distal His as a general acid–base catalyst by adjusting the precise location of the distal His as well as the basicity of the distal His through the His42–Asn70 hydrogen bond.

Effect of Ni^{2+} on Lifetime of the Enzyme

A previous study showed that increased functional stability of HRP, induced by activation concentration of Ni^{2+}, is associated with increasing conformational stability of the enzyme, $\Delta G^{\circ}_{(H_2O)}$, by 4.9 kJ/mol *(50)*.

In order to investigate the relationship among activatory effects, conformational stabilization, and long-term functional stability of HRP, the effect of Ni^{2+} (at activatory concentration) on the lifetime of the enzyme was investigated (*see* Fig. 4). Figure 4 shows that in the presence of activatory concentrations of Ni^{2+} (2 m*M*), the enzyme activity is increased and retained for a longer period of time compared to the native enzyme. From a biotechnological point of view, the long-term stability of HRP has great importance. Activation of the enzyme by metal ions confirms the idea that increased activity in the presence of metal ions is a result of specific binding

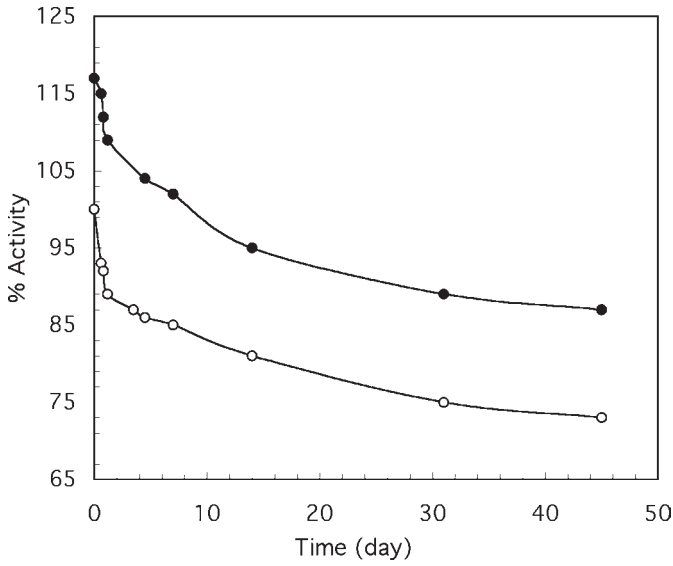

Fig. 4. Long-term stability of HRP induced by Ni^{2+} (2 m*M*). A HRP solution of 3×10^{-7} *M* was incubated with 2 m*M* of Ni^{2+} in 2.5 m*M* phosphate buffer of pH = 7.0 and 27°C. At given time intervals, 5 µL of incubated solution was used for activity measurements. Details of the enzyme assay are described in the Material and Methods section. ●, in the presence of Ni^{2+}; ○, without the presence of Ni^{2+}.

of metal ions to the protein, which, in turn, leads to formation of a "peroxidatic active site" parallel to the main active site of the enzyme (heme group) *(52,53)*. In other words, this type of M^{2+}–protein interaction results to a synergistic effect in the catalytic activity of the enzyme *(54)*.

Generally, metal ions can coordinate to active-site residues, leading to activation *(40)*. Conversely, such coordination may block substrate interaction, causing inhibition *(51)*. The pH-profile studies confirm the hypothesis that in the inhibitory region, in addition to histidine, Asp/Glu residues are also affected. This effect arises from the binding of metal ions (in higher concentration) to such residues. This process is associated with indirect perturbation of binding of AH (hydrogen donor) on its specific site leading to inhibition of the enzyme. A comparison of K_I values (*see* Table 2) shows that the inhibitory strengths are decreased as $Mn^{2+}>Co^{2+}>Ni^{2+}>Cu^{2+}$, which means that Mn^{2+} is the most powerful inhibitor in this set *(55)*.

Conclusion

The addition of nickel ion in the range of activatory concentration results in an increasing functional stability of HRP and stabilization of the enzyme structure along with its long-term stability, simultaneously. On the other hand, from a biotechnological point of view, care must be taken to avoid contamination of HRP solutions by small amounts of Co^{2+} and Cu^{2+} (in the range of their transition concentrations, $[D]_{1/2}$), because

these metal ions convert the HRP structure to a partially denatured form associated with inhibition of the enzyme.

References

1. Dunford, H. B. (1999), *Heme Peroxidases*, Wiley, New York.
2. Illenas, A. (1999), *Electron. J. Biotech.* **2,** 7–15.
3. Khajeh, K. and Nemat-Gorgani, M. (2001), *Appl. Biochem. Biotech.* **90**, 1–9.
4. Garcia, D. and Marty, J. (1998), *Appl. Biochem. Bioeng.* **73,** 173–184.
5. Triantafyllou, A., Wehtje, E., Adlercreutz, P., and Mattiasson, B. (1997), *Biotech. Bioeng.* **54,** 67–76.
6. Khajeh, K., Naderi-Manesh, H., Ranjbar, B., Moosavi-Movahedi, A. A., and Nemat-Gorgani, M. (2001), *Enzyme Microb. Technol.* **28,** 543–549.
7. Woodlock, A. F. and Harrap, B. S. (1968), *Aust. J. Biol. Sci.* **21,** 821–826.
8. Schleich, T. and von Hippel, P. H. (1970), *Biochemistry* **9,** 1059–1066.
9. Sipos, T. and Merkel, J. R. (1970), *Biochemistry* **9,** 2766–2775.
10. Wilson, R. H., Evans, H. J., and Becker, R. R. (1967), *J. Biol. Chem.* **242,** 3825–3832.
11. Von Hippel, P. H. and Wong, K. Y. (1965), *J. Biol. Chem.* **240,** 3909–3923.
12. Jpn. Kokai Tokkyo Koho JP07, 177,883 [95,177,833], 18 July 1995.
13. Holzbauer, I. E., English, A. M., and Ismail, A. A. (1996), *Biochemistry* **35,** 5488–5494.
14. Tsaprailis, G., Chan, D. W. S., and English, A. M. (1998), *Biochemistry* **37,** 2004–2016.
15. Moosavi-Movahedi, A. A., Nazari, K., and Saboury, A. A. (1997), *Colloids Surf. B: Biointerf.* **9,** 123–130.
16. Chattopadhyay, K. and Mazumdar, S. (2000), *Biochemistry* **39,** 263–270.
17. Haschke, R. H. and Friedhoff, J. M. (1978), *Biochem. Biophys. Res. Commun.* **80,** 1039–1042.
18. Ogawa, S., Shiro, Y., and Morishima, I. (1979), *Biochem. Biophys. Res. Commun.* **90,** 674–678.
19. Shiro, Y., Kurono, M., and Morishima, I. (1986), *J. Biol. Chem.* **261,** 9382–9390.
20. Morishima, I., Kurano, M., and Shiro, Y. (1986), *J. Biol. Chem.* **261,** 9391–9399.
21. Kaposi, A. D., Fidy, J., Manas, E. S., Vanderkooi, J. M., and Wright, W. W. (1999), *Biochim. Biophys. Acta* **1435,** 41–50.
22. Gajhede, M., Schuller, D. J., Henriksen, A., Smith, A. T., and Poulos, T. L. (1997), *Nat. Struct. Biol.* **4,** 1032–1038.
23. Smith, A. T., Santama, N., Dacey, S., Edwards, M., Bray, R. C., Thorneley, R. N. F., et al. (1990), *J. Biol. Chem.* **265,** 13,335–13,343.
24. Pahari, D., Patel, A. B., and Behere, D. V. (1995), *J. Inorg. Biochem.* **60,** 245–255.
25. Moosavi-Movahedi, A. A. and Nazari, K. (1995), *Int. J. Biol. Macromol.* **17,** 43–47.
26. Pappa, H. S. and Cass, A. E. G. (1993), *Eur. J. Biochem.* **212,** 227–235.
27. Smulevich, G., Feis, A., Indiani, C., Becucci, M., and Marzocchi, M. P. (1999), *J. Biol. Inorg. Chem.* **4,** 39–47.
28. Henriksen, A., Schuller, D. J., Meno, K., Welinder, K. G., Smith, A. T., and Gajhede, M. (1998), *Biochemistry* **37,** 8054–8060.
29. Brzyska, M., Ciêszczy, K., and £obarzewski, J. (1997), *J. Chem. Tech. Biotech.* **68,** 101–109.
30. Guilbault, G. G., Brignac, P., Jr., and Zimmer, M. (1968), *Anal. Chem.* **40,** 190–196.
31. Converso, D. A., Fernandez, M. E., and Tomaro, M. L. (2000), *J. Enzyme Inhib.* **15,** 171–183.
32. Youngs, H. L., Sundaramoorthy, M., and Gold, H. (2000), *Eur. J. Biochem.* **267,** 1761–1769.
33. Maehly, A. C. (1955), *Methods Enzymol.* **II,** 801–813.
34. Beer, R. F., Jr. and Sizer, I. W. (1952), *J. Biol. Chem.* **195,** 133–140.
35. Chauthaiwale, J. and Rao, M. (1994), *Biochim. Biophys. Acta* **1204,** 164–168.
36. Miles, E. W. (1977), *Methods Enzymol.* **47,** 431–442.
37. Pace, C. N., Shirley, B. A., Mcnutt, M., and Gajiwala, K. (1996), *FASEB J.* **10,** 75–83.

38. Pace, C. N. (1986), *Methods Enzymol.* **13,** 266–280.
39. Pace, C. N. (1990), *Trends Biochem. Sci.* **15,** 14–17.
40. Palmer, T. L. (1991), *Understanding Enzymes*, 3rd ed., Ellis Horwood, New York, pp. 139–212.
41. Farzami, B. (1992), *Metal Ions in Biology and Medicine*, (Anatussopoulou, U. Z. and Collery, P., eds.), John Libbey Eurotext, Paris, p. 102.
42. Farzami, B., Kuimov, A. N., and Kochetov, G. A. (1992), *J. Sci. I. R. Iran* **3,** 81–85.
43. Farzami, B., Moosavi-Movahedi, A. A., and Naderi, G. A. (1994), *Int. J. Biol. Macromol.* **16,** 181–186.
44. Modi, S. (1995), *Biometals* **8,** 218–222.
45. Farzami, B., Nazari, K., and Moosavi-Movahedi, A. A. (1997), *J. Sci. I. R. Iran* **8,** 209–216.
46. Rulisek, L. and Vondrasek, J. (1998), *J. Inorg. Biochem.* **71,** 115–127.
47. Welinder, K. G. (1985), *Eur. J. Biochem.* **151,** 497–504.
48. Polous, T. L. and Kraut, J. (1980), *J. Biol. Chem.* **225,** 8199–8205.
49. Rodriguez-Lopez, J. N., Smith, A. T., and Thorneley, R. N. F (1996), *J. Biol. Inorg. Chem.* **1,** 136–142.
50. Mahmoudi, A., Nazari, K., Moosavi-Movahedi, A. A., and Saboury, A. A. (2002), *Thermochimica Acta* **385,** 33–39.
51. Shi, X., Dalal, S., and Kasprzak, K. S. (1992), *Arch. Biochem. Biophys.* **299,** 154–162.
52. Dutta, A. K., Misra, M., North, S. L., and Kasprzak, K. S. (1992), *Carcinogenesis* **13,** 283–287.
53. Louie, A. Y. and Maede, T. J. (1999), *Chem. Rev.* **99,** 2711–2734.
54. Sigel, H. (1969), *Angew. Chem. Internat. Edit.* **8,** 167–177.
55. Hay, R. W. (1991), *Bio-Inorganic Chemistry*, Ellis Horwood, New York, p. 24.